Decision-Making Under Uncertainty on Preventive Actions Boosting Power Grid Resilience

Matthias Noebels, *Student Member, IEEE*, Jairo Quirós-Tortós, *Senior Member, IEEE*, and Mathaios Panteli, *Senior Member, IEEE*

***Abstract*—The growing impact of weather-related power outages on economy and society in the last decades underlines the rising need for power system resilience. Power system resilience can be boosted through adoption of probabilistic approaches and preventive actions building on smart grid capabilities. Decisions on the best-performing preventive action, however, are nontrivial and must consider the expected impact of an upcoming event, weather forecasts, fault probabilities, and their corresponding uncertainties. This article presents a three-stage decision-making methodology that is based on assessing weighted preevent and postevent performance loss and considers spatial uncertainty of fault probabilities, modeled by probability distributions. The methodology is demonstrated using preventive actions, such as additional network constraints and islanding, aiming to mitigate cascading failures in transmission networks. Their performance loss is compared to the traditional *N*-1 criterion. Simultaneous faults of up to three lines are considered as initiating cause in the IEEE 30-bus network and the 489-bus German transmission network to verify potential and scalability of the methodology. Results show that the decision-making methodology effectively identifies the best-performing action to reduce the risk of cascading failures for any level of uncertainty.**

***Index Terms*—Power system faults, power system modeling, power system reliability, power systems, resilience, risk analysis, transmission lines.**

I. Introduction

THE number of weather-related power outages has significantly increased during the last decades. Cascading failures belong to the main mechanisms behind large outages [1] and can, once triggered, affect vast areas and huge numbers of people [2], [3]. Consequently, the impact of power outages on economy and society has drawn attention to a rising need for power system resilience [4]. Traditional deterministic reliability criteria, such as *N*-1 or *N*-*k*, are becoming less effective to deal with the increasing stresses and shocks on power networks [5]. They would also require excessive and expensive safety margins to provide satisfying levels of resilience to extreme weather events, that are likely to damage several components simultaneously [6], [7]. Instead, probabilistic approaches gain increasing interest by the research community and network operators [8]–[10].

The shift toward probabilistic approaches requires addressing the presence of uncertainty. Sources of uncertainty include weather predictions, load forecast errors, monitoring errors, and physical system parameter estimation [11]. In [12], techniques for modeling uncertainty in power networks are reviewed, such as expressing uncertainty by using probability density functions. Network operators must consider these uncertainties when making decisions, both in long-term planning and short-term operation [13]. Examples include the risk-based security assessment of power systems that are exposed to threats such as natural hazards and malicious attacks [8], market prices [14], [15], and load and renewable generation forecasting [16], [17].

The range of potential operational measures increasing power network resilience that are reported in the literature is extensive [18], and includes, among others, preventive islanding [19], [20], microgrids [21], [22], storage [23], [24], topology reconfiguration [25], [26], and restoration planning [27], [28]. Recently, machine learning methods have gained increasing attention for fault prediction under extreme conditions and resilience enhancements [29]–[31]. The decision between different preventive actions requires dedicated metrics capturing the stochastic nature of power networks and extreme events, such as [32]. The metrics can then be used for resilience assessment and enhancement, e.g., by solving an optimization problem [33]–[35] or training of supervised machine learning algorithms [29], thus providing network operators with an effective decision strategy. However, results obtained from optimization are often only valid for a specific operating condition and provide little insights into the generalized, underlying principles of how such optimizations improve resilience. Machine learning requires a large number of training data, which is often obtained from computationally expensive Monte Carlo-simulations. Additionally, to the knowledge of the authors the uncertainty inherent in power systems and weather forecasts as well as the performance of preventive actions under varying levels and sources of uncertainty has not been adequately considered yet.

Manuscript received October 28, 2020; revised February 1, 2021 and May 26, 2021; accepted August 23, 2021. Date of publication October 5, 2021; date of current version June 13, 2022. This work was supported in part by the EPSRC under Grant EP/L016141/1 and Grant EP/R030294/1 through the Power Networks Centre for Doctoral Training and the Techno-Economic framework for Resilient and Sustainable Electrification (TERSE) project, and in part by the Newton Prize project "Resilient Planning of Low-Carbon Power Systems" (EPSRC) under Project 1304. *(Corresponding author: Mathaios Panteli.)*

Matthias Noebels is with the Department of Electrical and Electronic Engineering, University of Manchester Faculty of Science and Engineering, Manchester M13 9PL, U.K. (e-mail: matthias.noebels@manchester.ac.uk).

Jairo Quirós-Tortós is with the School of Electrical Engineering, Universidad de Costa Rica, San Pedro, Montes de Oca, UCR 11501-2060, Costa Rica (e-mail: jairoquirostortos@ieee.org).

Mathaios Panteli is with the Electrical and Electronic Engineering, University of Cyprus, Nicosia 1678, Cyprus (e-mail: panteli.mathaios@ucy.ac.cy).

Digital Object Identifier 10.1109/JSYST.2021.3108221

This article presents a risk assessment to weather-related power outages under spatial uncertainty and proposes a three-stage decision-making process aiding network operators on choosing the best-performing preventive action to improve power grid resilience. Spatial uncertainty results, for instance, from numerical weather predictions, and can be quantified by ensemble forecasting [36]. In particular, the key contributions of this article are as follows:

1) A novel quantification of performance loss considering weighted preevent and postevent performance loss caused by preventive actions as well as the uncertainty-based risk (Stage I).
2) A risk assessment of transmission line outages depending on spatial uncertainty in weather-related extreme events, obtained for individual combinations of line outages, avoiding Monte Carlo-simulations (Stage II).
3) A practical decision-making process, exemplified by look-up tables, for network operators to reach performance-driven decisions on preventive actions for an event, depending on spatial event uncertainty (Stage III).

The separation into three stages considers the computational complexity of the methodology, allowing more complex steps to be performed offline, and steps that need to consider quickly evolving and changing conditions online in real-time. The methodology, which is described in detail in Section II, is demonstrated in this article through three different preventive actions that are applied prior to wind storms and can mitigate their impact: Enforcing the *N*-1 criterion only for specific lines [5], isolating a single area from the main network [19], and sectionalizing the entire network into self-sustaining islands [20]. The methodology is not limited to these preventive actions or windstorms, but can be expanded to alternative actions or event types. All preventive actions considered here are compared to the traditional *N*-1 criterion. Results obtained from deploying the methodology on the IEEE 30-bus test network and the 489-bus German transmission network in Section III show how performance loss captures advantages and disadvantages of preventive actions, quantified via weighted pre-event and post-event performance loss, and ranks actions according to their performance for different levels of uncertainty. The proposed decision-making methodology, exemplified by look-up tables but expandable to more flexible machine learning algorithms, effectively identifies the best-performing action to reduce the risk of power outages caused by cascading failures, hence improving power grid resilience.

II. Methodology for Decision-Making on Preventive Actions Under Uncertainty

Fig. 1 shows the steps of the proposed performance-driven decision-making methodology for preventive actions under spatial uncertainty. As illustrated in the figure, the methodology can be split into three stages, relating to the timescales on which each stage can be performed. These timescales depend both on the computational complexity and the availability of required information to each stage. The steps necessary to undertake the

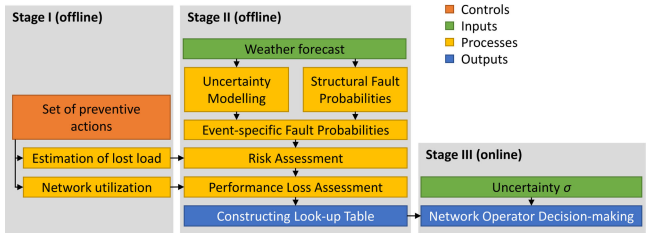

Fig. 1. Decision-making methodology for preventive actions.

methodology are described in detail in the following sections. In this article, the impact of windstorms on power grid resilience is analyzed, i.e., the occurrence of wind speeds related to force 10 and above on the Beaufort scale [37], for instance caused by low-pressure systems, hurricanes, or tornadoes. However, the methodology can also be applied to other hazards. Such hazards can lead to transmission line faults, e.g., due to physical damage or tree contact. This can result in cascading failures of power system assets, and potentially in the unintentional separation of the network into islands.

A. Uncertainty Modeling

Uncertainty significantly increases the complexity of decision-making, as it turns a trivial decision based on certainty into a nontrivial decision. Uncertainty is a result of imperfect knowledge about the power network as well as the upcoming event. Examples are load and weather forecast errors or monitoring errors. If a network operator is certain about the impact of an upcoming event, they can prepare the network for this specific impact, for instance by deactivating the affected part of the network or providing a backup strategy. As the uncertainty increases and a wider range of impacts becomes possible, the network operator needs to employ actions that effectively deal with this increased uncertainty whilst being potentially less cost-efficient. In any case, the decision-making needs to consider the level of uncertainty involved to provide power grid resilience under various conditions.

Uncertainty of weather forecasts can be quantified using ensemble forecasting [36]. Based on the forecast, the network operator can identify geographic areas in which the event is predicted to cause damage to the system and the probability for this to happen.

Decision-making under uncertainty requires a quantification of uncertainty [12]. In this article, uncertainty is a result of an increasing number of outcomes that an event can cause in a network, i.e., an increasing number of combinations of transmission lines that may fault. Mathematically, this *uncertainty* σ describes the radius of a circle around the location of the predicted event center $\boldsymbol{r}_0$, expressed by the following weight function:

$$f(\boldsymbol{r},\sigma)=\begin{cases}1, & \text{if } ||\boldsymbol{r}-\boldsymbol{r}_0||\leq\sigma\\ 0, & \text{otherwise.}\end{cases} \tag{1}$$

Transmission lines within this circle can be affected by the event, while transmission lines outside of this circle are assumed to be safe. σ can thus be interpreted as the imperfect knowledge

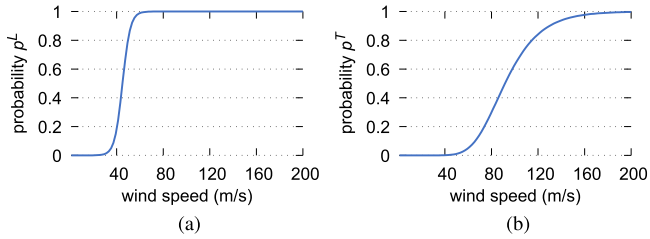

Fig. 2. Wind fragility curves [19]. (a) Line fragility curve per 100 km. (b) Tower fragility curve.

of the predicted location of an event. If the uncertainty is low, there is only a small number of event outcomes. The network can then be prepared in a way that works best for this specific event outcome but which would not be suitable for any other event outcome. If the uncertainty is high, there is a large number of event outcomes, and the network needs to be prepared in a way that works well for a wide range of event outcomes, e.g., combinations of transmission line faults.

B. Structural Fault Probability for Wind Storms

The probabilities of possible combinations of event outcomes, e.g., transmission line faults, need to consider the physical characteristics, e.g., the length, of the transmission lines. The *structural fault probability* of an overhead line is obtained from fragility curves, that describe its fault probability for a given environmental parameter, such as wind speed. Fragility curves can be obtained for various hazards such as windstorms, flooding, wildfires or earthquakes, and hence the methodology is not limited to a specific hazard. Fragility curves are usually extracted from outage statistics and make no assumption about the actual reason for a fault. They thus consider all types of faults that can be related to the respective hazard, including, but not limited to, tree contact, line-to-line faults, or conductor break [38]. In this article, the fragility curves $p^L(v_w)$ and $p^T(v_w)$ (see Fig. 2) give the fault probabilities of a line segment and tower, respectively, for windstorms, depending on the occurring wind speed. It is assumed that the fault of any tower or line segment in a line leads to a fault of the entire line. It is further assumed that structural faults of overhead lines are independent events, i.e., overhead lines are separated far enough from each other so that the structural fault of one line has no immediate effect on other lines. Note that this only relates to structural faults. Cascading failures due to successive overloading are handled in Section II-F.

The total structural fault probability $p_{l,\text{struct}}$ of a line of length L_l at wind speed v_w is

$$p_{\text{struct}}(L_l, v_w) = p_l^L(L_l, v_w) + p_l^T(L_l, v_w) - p_l^L(L_l, v_w) \cdot p_l^T(L_l, v_w) \tag{2}$$

where p_l^L and p_l^T are the failure probabilities of the entire line and all towers in the line, respectively. Assuming, without loss of generality, line segments of length 100 km, p_l^L can be calculated by

$$p_l^L(L_l, v_w) = 1 - \left(1 - p^L(v_w)\right)^{\frac{L_l}{100\,\text{km}}}. \tag{3}$$

With Δ_T the distance between two towers, $p_{n,m}^T$ can be calculated by

$$p_l^T(L_l, v_w) = 1 - \left(1 - p^T(v_w)\right)^{\frac{L_l}{\Delta_T}}. \tag{4}$$

C. Event-Specific Fault Probability

Because some lines might only fall partially within the uncertainty radius defined by σ, the *event-specific fault probability*

$$p_{l,\text{event}}(\sigma) = p_{\text{struct}}(\hat{L}_l(\sigma)) \tag{5}$$

of line l uses the effective length $\hat{L}_l(\sigma)$ of a transmission line, i.e., the length of the line that falls within the uncertainty radius, instead of the physical line length L_l. This reduces the probability of lines that fall only partially within the uncertainty radius. Given the weight function (1), the effective length can be calculated using a line integral

$$\hat{L}_l(\sigma) = \int_{\gamma_l} f(\gamma_l, \sigma)\mathrm{d}s. \tag{6}$$

Here, $\gamma_l : \mathbb{R} \to \mathbb{R}^2$ is a parametrization of the path of the line with path parameter s. In this study, lines are assumed to form straight connections between their end buses, which simplifies calculating the line integral in (6). If detailed information about the run of the lines is available, the path function can be any other nonclosed path.

D. Probability of Simultaneous Faults

Based on the event-specific fault probabilities of lines, the *probability of a simultaneous fault* of any combination of lines can be calculated. The survival probability P_0, i.e., the probability that no line fault occurs, is given by

$$P_0 = \prod_{l \in \Lambda} (1 - p_l). \tag{7}$$

Thus, the probability of an *N*-1 contingency of line l is

$$p_{l,1} = p_l \cdot \frac{P_0}{1 - p_l}. \tag{8}$$

Note that an *N*-1 contingency implies that no fault occurs for all lines except line l. In general, the probability of an *N*-k contingency of a combination of lines $\lambda \subset \Lambda$ is

$$p_{\lambda,k} = P_0 \cdot \prod_{l \in \lambda} \frac{p_l}{1 - p_l}. \tag{9}$$

The total probability $\overline{p}_k$ of an *N*-k contingency can be obtained by summing the fault probabilities of all $\binom{\Lambda}{k}$ combinations of lines that make up for this contingency. For example, the total probability of an *N*-1 contingency is

$$\overline{p}_1 = \sum_{l \in \Lambda} p_{l,1} \tag{10}$$

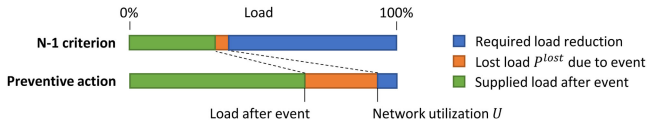

Fig. 3. Network utilization and lost load.

In general, the total probability of an N-k contingency is

$$\overline{p}_k = \sum_{\lambda \subset \binom{\Lambda}{k}} p_{\lambda,k} \tag{11}$$

with $\binom{\Lambda}{k}$ the set of all k-combinations of lines.

E. Network Utilization and Preventive Actions

Under normal conditions, a network supplies loads up to its *network utilization* U, which is in this context a measure for the maximum load that can be supplied for a given set of *network constraints*. Different units can be used to express U, e.g., MW or MWh, if the duration of the event is known. To become independent on the choice of unit and also allow for comparison between different networks and network loadings, in the following U is expressed as a percentage of the total network load, i.e., peak load. A network utilization of 100% means that all loads are supplied and there is no load shedding. A network utilization of 0% means that all loads are fully shed. Network constraints are any limitations on the use of the network and its components, e.g., the available generation capacity, deactivated transmission lines or line ratings. The network is generally fully utilized ($U = 100\%$), if the only network constraints considered are generation capacity and line ratings. Note that within this context network utilization makes no assumption on the availability or status of transmission lines.

Traditionally, security of supply is ensured by applying the N-1 criterion. This adds further constraints and thus significantly reduces the network utilization U (see Fig. 3). Lost load P^{lost} in case of the loss of a single component should be zero, however, lost load can still be caused by the loss of two or more lines.

A *preventive action* is an operational measure that, contrary to the N-1 criterion, temporarily modifies the network constraints before an event causes severe degradation to the network. Network constraints include, for instance, temporarily redispatching loads and generators or reconfiguring the network. These are achieved by using existing smart grid capabilities and require no additional investments in bulk electrical power infrastructure. A preventive action may temporarily reduce the network utilization U, which can, for instance, be achieved through controllable demand management (e.g., switching off big industrial or commercial loads).

The decision between the N-1 criterion and various preventive actions can be based on a performance loss analysis and requires a tradeoff between the preevent performance loss $\psi^{\text{pre},\alpha}$ and postevent performance loss $\psi^{\text{post},\alpha}$, where α denotes the action. The preevent performance loss $\psi^{\text{pre},\alpha}$ of an action includes the impact that is incurred by the network constraints it comes with, e.g., reductions in network utilization, generator dispatching, number of switching actions, or any other impact that may come with applying the action. Through online monitoring, e.g., via phasor measurement units, $\psi^{\text{pre},\alpha}$ can in principle be accurately determined. The postevent performance loss $\psi^{\text{post},\alpha}$ of an action includes the risk that is incurred by the event, e.g., any lost load that would lead to compensations the network operator might be liable to pay to disconnected customers. The accuracy of $\psi^{\text{post},\alpha}$ depends largely on the method used to predict the performance loss (c.f. Section II-F), but can also be increased through better knowledge of the preevent system state.

The following presents the actions that are analyzed and compared in this article:

1) N-1 and 1-1 Criterion: The traditional deterministic N-1 criterion requires that any individual fault of one of the N components (e.g., lines) in the system must not lead to load curtailments. An N-1 secure dispatch can be obtained from security-constrained optimal power flow solvers. In order to meet the N-1 criterion, large safety margins have to be introduced and the network utilization is generally reduced. Hence, the preevent performance loss $\psi^{\text{pre},\alpha}$ is large, but for individual faults the postevent performance loss $\psi^{\text{post},\alpha}$ is zero.

The N-1 criterion is deterministic as it treats every component the same, independent of its actual fault probability. It becomes probabilistic, if it is only applied to specific lines. In this article, an 1-1 criterion is demonstrated and evaluated, which means that load curtailments are only prevented in case of the loss of a single line. This relaxation of constraints can lead to a reduction of the preevent performance loss $\psi^{\text{pre},\alpha}$, but the postevent performance loss $\psi^{\text{post},\alpha}$ may be increased if lines other than the specified line are affected.

2) Isolating and Islanding: Faults can be contained within a part of the network if this part is isolated from the remaining network in an island. Islanding the network is an intentional action by the network operator, and the network operator can decide on the number of islands to be created and their extent. Such an intentional islanding scheme to prevent cascading failures caused by extreme weather is proposed in [19]. With increasing number of islands, the impact of cascading failures generally decreases, as it is shown in [20], even when the N-1 criterion is not maintained in the individual islands. Network utilization generally decreases with increasing number of islands, as some islands might not have sufficient generation capacity to supply all their loads. This means an increasing preevent performance loss $\psi^{\text{pre},\alpha}$ for increasing number of islands, but a decreasing postevent performance loss $\psi^{\text{post},\alpha}$. However, since the N-1 criterion does not necessarily have to be applied, the preevent performance loss $\psi^{\text{pre},\alpha}$ for islanding can still be less than for the N-1 criterion.

Different methods exist in the literature to obtain the parts of the network to be included in the island while optimizing the network utilization. One of them is spectral clustering, which is widely used in the literature for islanding power networks [39]–[41]. Spectral clustering can either be used to isolate areas from the remaining network, or to sectionalize the entire network into approximately equal-sized islands. Both options are demonstrated and evaluated in this article.

$w_{pre}=1$, $w_{post}=1$	Network utilization U		
Risk R	100%	50%	0%
0%	0	0.5	1
50%	0.5	0.75	1
100%	1	1	1

$w_{pre}=2$, $w_{post}=1$	Network utilization U		
Risk R	100%	50%	0%
0%	0	1	2
50%	0.5	1.25	2
100%	1	1.5	2

$w_{pre}=1$, $w_{post}=2$	Network utilization U		
Risk R	100%	50%	0%
0%	0	0.5	1
50%	1	1	1
100%	2	1.5	1

Fig. 4. Performance loss depending on network utilization and risk for different values of w_{pre} and w_{post}.

F. Estimation of Lost Load

The unintentional, unplanned loss of a component of the network, such as a line, generator, substation, or load, due to an event can trigger subsequent tripping of other components, which were not initially affected by the event (cascading failure). This can cause further overloading of other lines, lead to instabilities and eventually entirely disconnected areas.

Various cascading failure models are described in the literature [42]. In this study, the static dc-based model described in [20] is used, which incorporates two main failure modes as follows.

1) If the power flow in a line exceeds the line's rating, the line is tripped.
2) If this has led to disintegration of the network into islanded areas, an island trips if there is a imbalance between generation and demand larger than a tolerance factor δ. This simulates the limited ability of generators and loads to adjust their power output and input, respectively, within a very short time. The impact of δ is studied in [20].

The power flow within the network is repeatedly calculated and tested for these two failure modes, until the power flow satisfies all constraints and the cascading failure is said to have come to a halt. The cascading failure model then returns the lost load $P_{\lambda}^{\text{lost}}$ caused by a set of faulted lines λ as a percentage of network utilization.

Estimating the lost load caused by a fault of every line is the computationally expensive part of this methodology. Particularly, if larger numbers of simultaneous faults should be considered, it may be not feasible to calculate the lost load for every possible combination. However, estimation of lost load for each combination depends solely on network topology, network constraints as required by the application of preventive actions, generator dispatch, and demand, which is available from load forecasting. The calculations can thus be performed offline, well ahead of an event (Stage I in Fig. 1). Once more information about the event is available, for example from weather forecasts, subsequent risk and performance loss assessment can be performed on a much shorter timescale (Stages II and III).

G. Risk and Performance Loss Assessment, Look-Up Tables

As discussed in Section II-E, the decision on preventive actions requires a tradeoff between pre- and postevent performance loss. The proposed performance loss assessment requires identification of the action α that leads to a minimum total performance loss

$$\psi^{\alpha} = w_{\text{pre}}\psi^{\text{pre},\alpha} + w_{\text{post}}\psi^{\text{post},\alpha} \tag{12}$$

where w_{pre} and w_{post} are weighting factors, which reflect the different influence that the pre- and postevent performance loss may have on decision making. For instance, in a scenario, where the value of lost load significantly exceeds the cost for preevent demand management, a network operator might decide to weight the postevent performance loss with a larger factor. This will drive the network operator to the action that has the highest positive influence on postevent performance loss. The unit and range of the weighting factors are not restricted and could, for instance, be expressed as a monetary value (e.g., value of lost load in \$/MWh, $\psi^{\text{pre},\alpha}$ and $\psi^{\text{post},\alpha}$ given in MWh). In this case, ψ^{α} would represent a financial loss.

In this article, $\psi^{\text{pre},\alpha}$ is determined by the reduction in network utilization $1-U$, and $\psi^{\text{post},\alpha}$ is determined by the *risk* R_k^{α} of an N-k contingency

$$R_k^{\alpha}(\sigma) = \frac{1}{\overline{p}_k} \sum_{\lambda \subset \binom{\Lambda}{k}} p_{\lambda,k}(\sigma) \cdot P_{\lambda}^{\text{lost},\alpha} \tag{13}$$

where $P_{\lambda}^{\text{lost},\alpha}$ is given as a percentage of network utilization. Note that the division by $\overline{p}_k$ normalizes the fault probabilities and conditions that an N-k contingency occurs. By doing so, the risk of each contingency size can be assessed independent of the event properties, i.e., the wind speed and storm radius. Equation (13) corresponds to a risk analysis based on the multiplication of the probability $p_{\lambda,k}(\sigma)$ of a line fault with the impact of this line fault, expressed by the lost load $P_{\lambda}^{\text{lost},\alpha}$ it causes. If $P_{\lambda}^{\text{lost},\alpha}$ is expressed as a percentage of the network utilization, R_k^{α} becomes unit-less. The sum over λ considers all possible combinations of N-k contingencies.

These considerations lead to the *performance loss* ψ

$$\psi_k^{\alpha}(\sigma) = w_{\text{pre}}(1-U^{\alpha}) + w_{\text{post}}R_k^{\alpha}(\sigma)U^{\alpha}. \tag{14}$$

R_k^{α} is multiplied with U^{α} because it was previously defined as a ratio of the network utilization. The relation of performance loss to network utilization and risk is visualized for different exemplary values of w_{pre} and w_{post} in Fig. 4. A performance loss of zero can only be reached if both the network utilization is 100% and the risk is 0%. If w_{pre} is larger than w_{post}, a decrease in network utilization leads to a larger performance loss than the same increase in risk. If w_{post} is larger than w_{pre}, an increase in risk leads to a larger performance loss then same decrease in network utilization. Note that the chosen weights in Fig. 4 are for demonstration purposes only, and their unit and range is not restricted by the methodology. In practice, w_{pre} and w_{post} would most likely be predetermined costs representing, for instance, demand response tariffs and the value of lost load, respectively.

H. Decision-Making via Look-Up Tables or Machine Learning

Comparing the performance loss of different preventive actions can efficiently aid network operators to identify the best-performing preventive action, i.e., the preventive action with the lowest performance loss, depending on the spatial uncertainty σ and the weighting factors w_{pre} and w_{post}. Particularly look-up tables, that define uncertainty ranges and assign a best-performing preventive action to each uncertainty range, are a simple yet powerful way for real-time decision making. Examples for such look-up tables are provided in Section III.

Alternatively to look-up tables, the performance loss can be used in a formal optimisation framework, or to train machine learning algorithms, e.g., decision trees, support vector machines, neural networks or another classifier returning the best-performing action for a set of predictors, such as uncertainty and other event parameters. To do so, training data must be obtained from simulations for a range of different preventive actions and event uncertainties. Note that the previous impact assessment in Section II-F (Stage I in Fig. 1) does not have to be repeated for different events, because it already captures all possible combinations of line faults. However, it would have to be repeated for different preventive actions, i.e., if a different area is to be isolated. After obtaining the training data and training the machine learning algorithm (Stage II), the algorithm can be used for real-time decision making without the need for further simulations (Stage III).

I. Exemplary Implementation

To summarize the key steps of the proposed uncertainty-based decision-making methodology (see Sections II-A and II-H), an exemplary implementation of the methodology following Fig. 1 is provided in Algorithm 1.

Algorithm 1 Uncertainty-based decision-making

Input: Contingency size k, pre- and post-event weights w_{pre}, w_{post}, set of actions A, set of uncertainties S
Output: Look-up table with best-performing action a for every σ

Determine all k-combinations of lines
▷ *Network utilization and lost load (Stage I):*
for all actions $a \in A$ **do**
  Calculate network utilization U^{α}
  for all k-combinations of lines λ **do**
    Calculate lost load $P_{\lambda}^{\text{lost},\alpha}$
  end for
end for
for all uncertainties $\sigma \in S$ **do**
  ▷ *Event-specific fault probabilities (Stage II):*
  for all k-combinations of lines λ **do**
    Calculate $p_{\lambda,k}(\sigma)$ (9)
    end for
    Calculate $\overline{p}_k(\sigma)$ (11)
    for all actions $\alpha \in A$ **do**
    ▷ *Risk assessment:*
      Calculate $R_k^{\alpha}(\sigma)$ (13)
    ▷ *Performance loss assessment:*
      Calculate $\psi_k^{\alpha}(\sigma)$ (14)
    end for
    Identify best-performing action $\hat{a}(\sigma) = \arg\min_a \psi_k^{\alpha}(\sigma)$
end for
▷ *Constructing look-up table:*
Return mapping $\sigma \mapsto \hat{a}(\sigma)$

III. Simulation Results

The methodology presented above is demonstrated on two different networks, the IEEE 30-bus test network (see Section III-A) and a 489-bus model of the German transmission network (see Section III-B). For each network, first the impact of line outages is evaluated, and then a risk and performance loss analysis for the preventive actions introduced in Section II-E is undertaken.

A. IEEE 30-Bus Test Network

The methodology is first demonstrated on a modified version of the IEEE 30-bus test network (see Fig. 5) to simulate stressed network conditions. The coordinates and distances of buses are arbitrarily assigned. Loads and generators are assigned randomly to the buses of the network, so that every bus has a load connected, and 50% of the buses have a generator connected (c.f. Table III). Line ratings are set to 150% of the initial power flow. The following analysis would be equivalent for other bus coordinates, ratios of generating buses or line ratings.

1) Lost Load: The color coding of each line λ in Fig. 5 indicates the lost load $P_{\lambda}^{\text{lost}}$ caused in the network when this line is lost. Losing line 25–27, for example, leads to overloading of the alternative lines in the ring connecting buses 25 and 27, which subsequently causes serious disintegration of the network and leads eventually to a lost load of 62%.

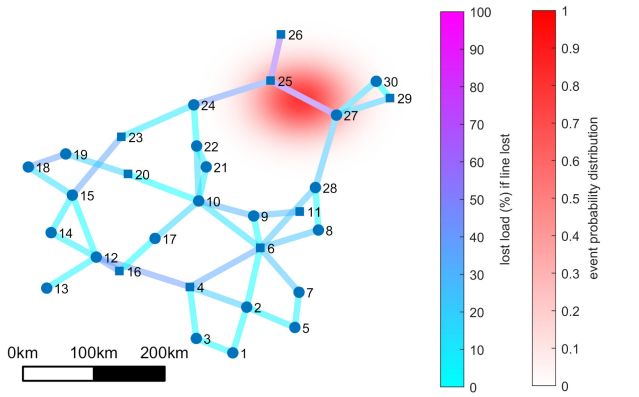

Fig. 5. Lost load $P_{\lambda}^{\text{lost}}$ caused by single line faults in the IEEE 30-bus test network, indicated by the color coding. The red shaded area indicates an event centered at line 25–27.

The lost load caused by a simultaneous fault of two lines can be taken from the color coding of each combination of lines in Fig. 6. Any combination of lines, whose individual

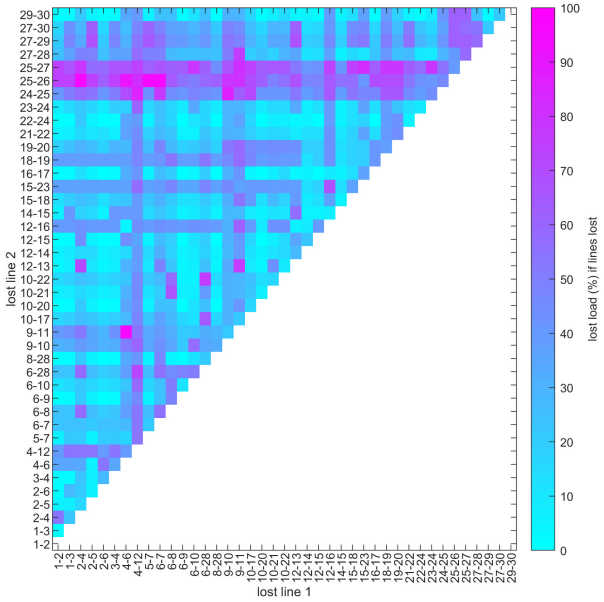

Fig. 6. Lost load $P_{\lambda}^{\text{lost}}$ caused by simultaneous fault of two lines in the IEEE 30-bus test network, indicated by the color coding.

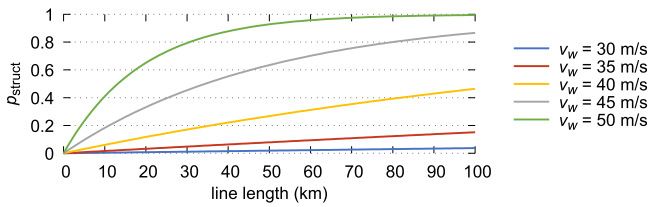

Fig. 7. Structural fault probability of an overhead line for different wind speeds depending on line length.

fault is already critical, has a large impact, but there are also certain combinations, which lead to a much larger impact than the combined individual fault would have. This indicates that certain combinations of line faults worsen the propagation of fault cascades in the network. Examples of those combinations, which have a large combined impact, are 4–6 and 9–11 ($P^{\text{lost}} = 96.8\%$), 2–4 and 12–13 ($P^{\text{lost}} = 70.5\%$), and 18–19 and 25–27 ($P^{\text{lost}} = 78.8\%$).

In a similar way, the lost load for a simultaneous fault of any number of lines can be determined.

2) Fault Probabilities: The dependency of structural fault probability of an overhead line on wind speed and line length is illustrated in Fig. 7 for a tower spacing of $\Delta t = 300$ m.

For this analysis, a windstorm centered at line 25–27 is chosen (highlighted in Fig. 5), as this is the worst case. The analysis would be equivalent for any other event center. Based on this event center, the probabilities of different contingencies can be calculated using (11), assuming, without loss of generality, a circular storm with constant wind speed over the entire area affected. For low wind speeds and small storm radii, the occurrence of no contingency at all is most probable (see Fig. 8). With increasing wind speed and storm radius, first N-1 contingencies become most likely, followed by N-2 and N-3 contingencies.

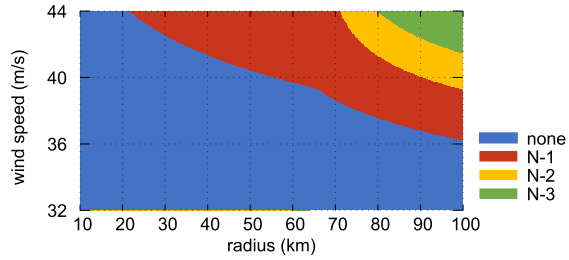

Fig. 8. Dominating contingency in the IEEE 30-bus test network depending on wind speed and storm radius.

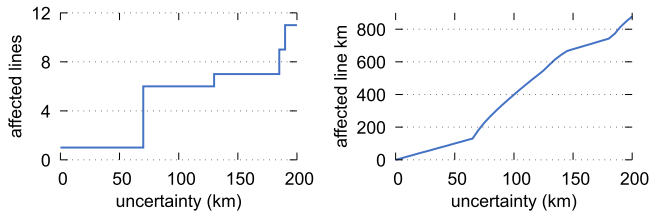

Fig. 9. Effect of uncertainty on number of fault combinations.

TABLE I
NETWORK UTILIZATION OF THE IEEE 30-BUS TEST NETWORK

Action	N-1	1-1	Isolating vulnerable area	Islanding
U (%)	26.2	90.8	99.1	94.5

3) Uncertainty: With increasing uncertainty, both the number of lines that can be affected by the event and the affected line kilometers, i.e., the total length of lines within the event area, increase (see Fig. 9(a) and (b)). Hence, also the number of combinations $\binom{\Lambda}{k}$ in (11) increases for larger uncertainties. As some lines may only be partially affected by an event, and the structural fault probabilities of overhead lines depend in this study only on the line length for a fixed wind speed, the affected line kilometers provide a more accurate view on the effect of increasing uncertainty.

4) Preventive Actions: The following three preventive actions are considered in this study and compared to the traditional N-1 criterion: the 1-1 criterion applied to line 25–27; isolating a single area around buses 25 and 27; and sectionalizing the network into four islands. The optimum number of islands depends on various factors, including the amount of generation and the desired level of resilience, as discussed in Section II-E. Previous work on this network suggests separation into four islands [20], leaving no isolated or disconnected buses, but other numbers of islands could have been chosen as well. Preventive actions increase the network utilization significantly compared to the traditional N-1 criterion (see Table I).

Fig. 10 shows the network topology after each preventive action. The color coding of each line indicates the lost load caused by its individual fault. The 1–1 criterion eliminates any impact of a loss of line 25–27, but the impact of a loss of other lines, such as 4–12 and 5–7, increases significantly. Isolating a single area not only significantly reduces the impact of the lines

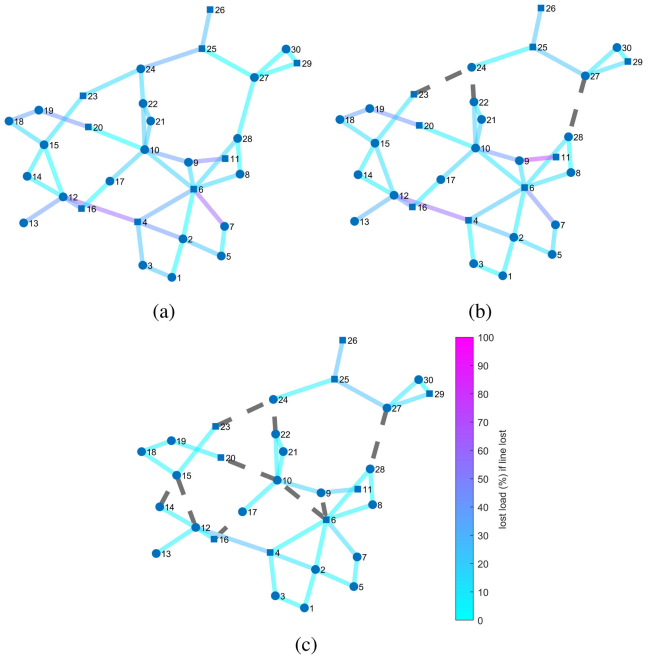

Fig. 10. Lost load P^{lost} caused by single line faults in the IEEE 30-bus test network for different preventive actions. (a) 1–1 criterion for line 25–27. (b) Isolated single area around bus 25. (c) Sectionalized into four islands.

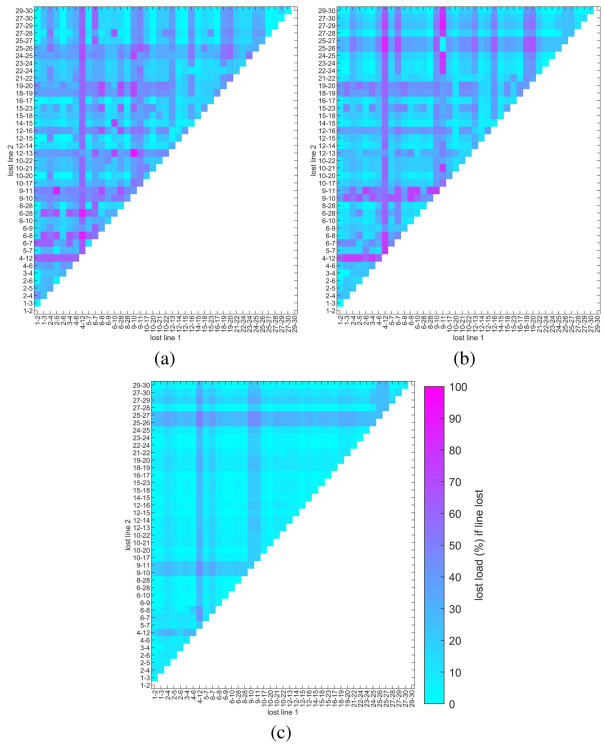

Fig. 11. Lost load P^{lost} caused by the simultaneous fault of two lines in the IEEE 30-bus test network for different preventive actions. (a) 1–1 criterion to line 25–27. (b) Isolated single area around bus 25. (c) Sectionalized into four islands.

within the area, but the measure is also extremely efficient in terms of network utilization (see Table I). Islanding reduces the lost load for every single line fault.

For the same preventive actions, the lost load caused by the simultaneous fault of any combinations of two lines can be calculated (see Fig. 11). Buses belonging to the same island can be observed as clustering in Fig. 11(b) and (c).

5) Performance Loss Assessment: Having determined fault probabilities and lost load for all preventive actions, the performance loss of each action can be calculated with (14) for every contingency size. For the calculation of fault probabilities, wind speed is now assumed to be 30 m/s, but this has only a very small impact on the risk of a given contingency because of the normalization of fault probabilities in (13). This may seem counterintuitive, however, it should be kept in mind that while wind speed has a large effect on contingency size, it affects structural fault probabilities of all affected lines in a very similar way. The analysis is undertaken for different values for w_{pre} and w_{post} (see Fig. 12). In case of an N-1 contingency, a preventive action can be found that leads to a lower performance loss than the N-1 criterion for every uncertainty σ in the considered range. As it can be expected, the performance loss of the N-1 criterion is independent of σ. Varying w_{pre} and w_{post} causes a narrowing or extending of the uncertainty ranges in which preventive actions lead to the lowest performance loss. If w_{pre} is larger than w_{post}, preventive actions that have a lower preevent performance loss are favored over a wider uncertainty range, in this case isolating a single area which has the highest network utilization (see Table I). The values of ψ for the N-1 criterion exceed 1 in this case and are not shown in the figure. If w_{post} is larger than w_{pre}, preventive actions that have a lower postevent performance loss are favored over a wider uncertainty range, in this case the 1–1 criterion or islanding (see Fig. 10). For the given fault probability distribution, the assessment can lead to a look-up table as visualized in Fig. 13, which can be used by the network operator to select the best-performing preventive action under different levels of spatial uncertainty.

Similarly, the performance loss of preventive actions in case of N-2 and N-3 contingencies can be assessed. Because the event center remains unchanged, the set of preventive actions is the same as for the N-1 case. The results for N-2 and N-3 contingencies reveal two trends: First, assuming larger contingency sizes increases the performance loss independent of the chosen action (see Fig. 12). Second, the range in which isolating a single area performs best shifts slightly toward smaller uncertainties for larger contingency sizes (see Fig. 13). Both trends can be related to the generally higher lost loads caused by the simultaneous fault of multiple lines while the network utilization remains unchanged. The performance loss of the N-1 criterion shows only a small dependency on σ, because its network utilization is so low that even most simultaneous faults do not cause significant lost load.

B. German Transmission Network

The methodology is also tested on the German transmission network (see Fig. 14), as provided by the SciGRID project [43], to demonstrate its scalability. Loads and generators are taken

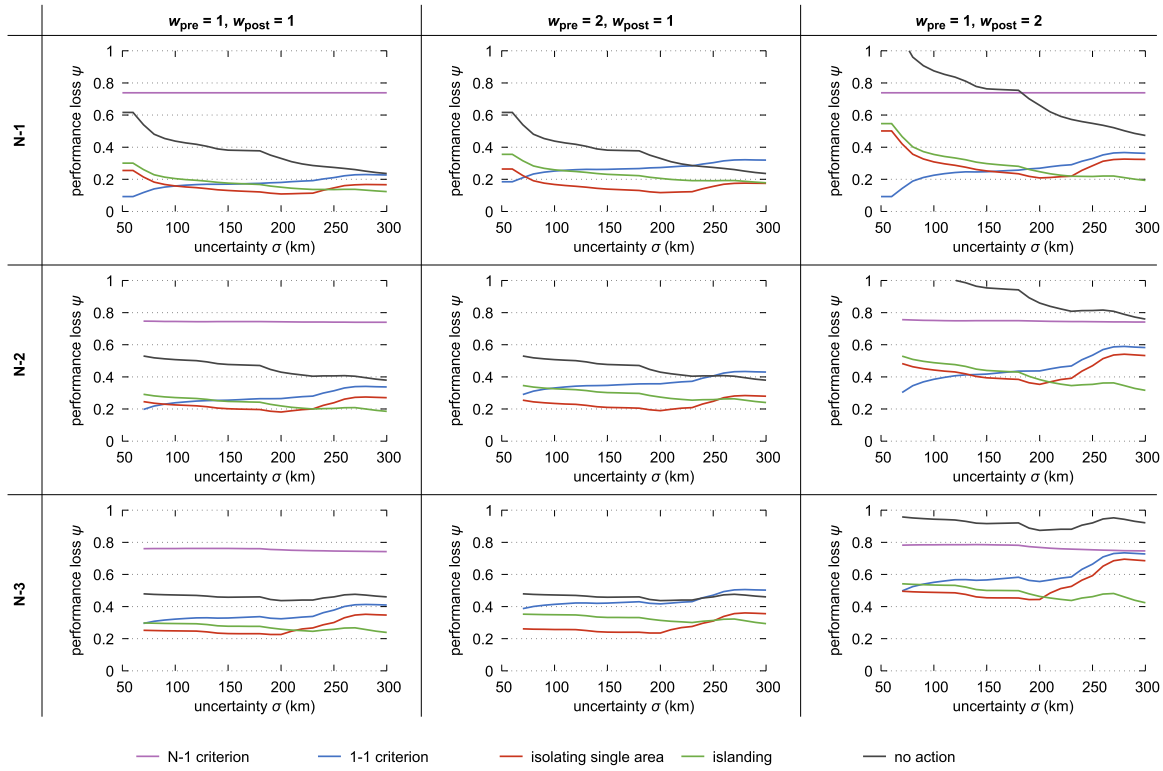

Fig. 12. Performance loss ψ in the IEEE 30-bus test network. Where the curve for the N-1 criterion cannot be seen, it exceeds a value of 1.

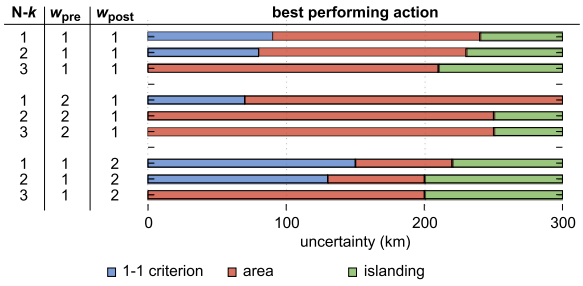

Fig. 13. Visualization of a look-up table for the IEEE 30-bus test network, giving the best performing action for each uncertainty range.

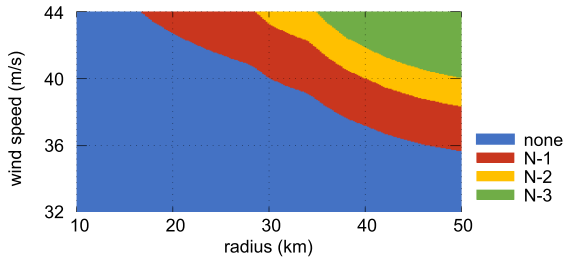

Fig. 15. Dominating contingency in the German transmission network depending on wind speed and storm radius.

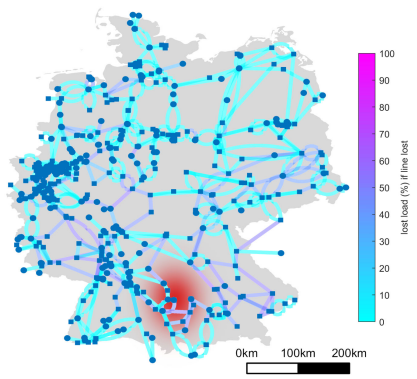

Fig. 14. Lost load $P_{\lambda}^{\text{lost}}$ caused by single line faults in the German transmission network, indicated by the color coding. The red shaded area indicates the location of an event centered at line 396–410.

from snapshots provided by the PyPSA toolbox [44], however, loads are scaled up to a total load of 87 GW for a network utilization of 100%. The network, reduced to the high and extra high voltage level, consists of 489 buses, 441 generators and 825 lines.

The color coding of each line λ in Fig. 14 indicates the lost load $P_{\lambda}^{\text{lost}}$ caused in the network when this line is lost. The lost load caused by the simultaneous fault of two lines is calculated as well but not shown here in this article.

An event centered at line 396–410 is chosen, as this is one of the worst cases (location indicated in Fig. 14). Similar to the IEEE 30-bus test network, the dominating contingency size increases with increasing wind speed and storm radius, however, larger contingencies are already dominating at lower radii (see Fig. 15). This is due to the much higher density of buses and lines.

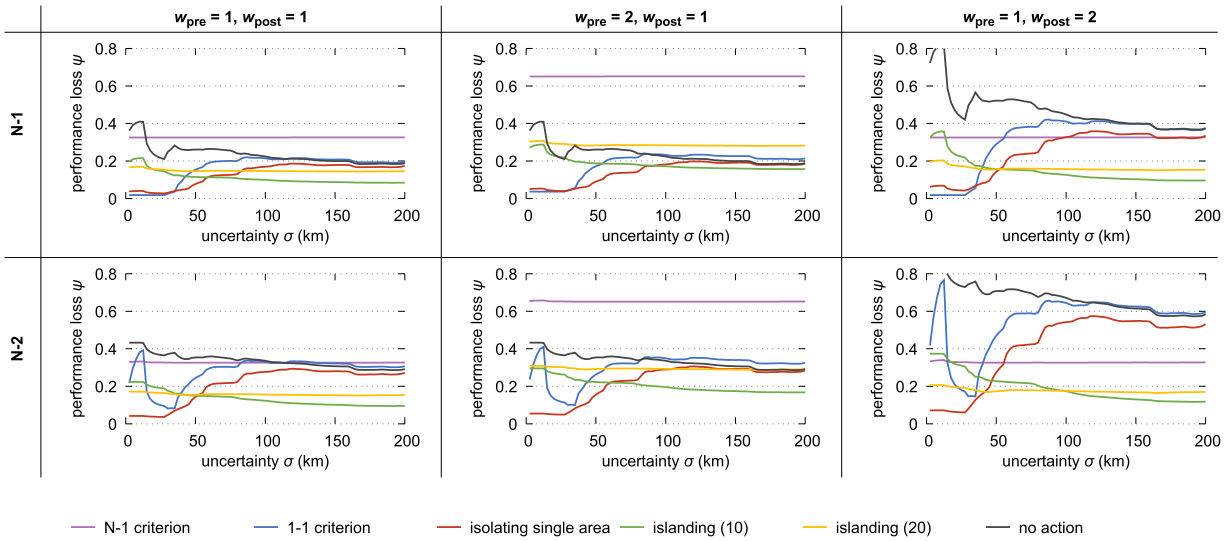

Fig. 16. Performance loss ψ in the German transmission network.

TABLE II
NETWORK UTILIZATION OF THE GERMAN TRANSMISSION NETWORK

Action	N-1	1-1	Isolating single area	Islanding	
				10	20
U (%)	67.5	98.2	98.8	92.7	86.3

TABLE III
MODIFICATIONS TO IEEE 30-BUS TEST NETWORK

Bus	Gen. (MW)	Load (MW)	Bus	Gen. (MW)	Load (MW)
1	-	36.0	16	52.8	12.3
2	-	18.9	17	-	50.4
3	-	0.1	18	-	34.7
4	287.2	31.6	19	-	9.2
5	-	70.0	20	82.5	14.8
6	281.0	62.5	21	-	19.8
7	-	54.3	22	-	67.2
8	-	43.9	23	73.0	43.2
9	-	28.7	24	-	69.4
10	-	50.2	25	46.3	25.7
11	245.8	76.2	26	218.7	1.0
12	-	76.2	27	-	53.2
13	-	57.6	28	-	27.9
14	-	74.8	29	72.5	94.6
15	-	64.5	30	-	90.6

The preventive actions considered are applying the 1–1 criterion to line 396–410, isolating a single area around buses 396 and 410, and islanding. Isolating a single area forms an island of 11 buses. Two different ways of islanding are compared (10 and 20 islands) to demonstrate the effect of island size, although other numbers of islands could have been chosen as well. Preventive actions increase the network utilization significantly compared to the N-1 criterion (see Table II). The N-1 criterion reduces network utilization by the most (32.5%). Both the 1–1 criterion and isolating a single area lead to a reduction in network utilization of only 1.8% and 1.2%, respectively. Creating 20 islands reduces network utilization more (13.7%) than creating 10 islands (7.3%), because with increasing number of islands, some islands do not have sufficient generation to supply all their loads.

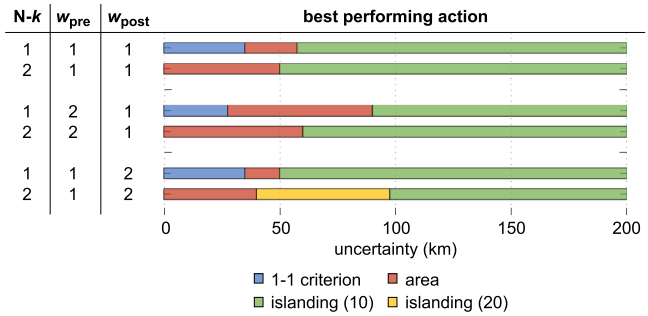

Fig. 17. Visualization of a look-up table for the German transmission network, giving the best performing action for each uncertainty range.

Having determined fault probabilities and lost load for all preventive actions, the performance loss of each action can be assessed based on (14) and similarly to the analysis in Section III-A (see Fig. 16). As expected, the performance loss of the N-1 criterion shows no dependency on σ for N-1 contingencies and only small dependency on σ for N-2 contingencies. However, there is again for every uncertainty a preventive action that performs better than the N-1 criterion. The resulting look-up table, that gives the best-performing preventive action for any uncertainty, is visualized in Fig. 17. By increasing w_{pre}, isolating a single area becomes preferred over a wider uncertainty range as it has the highest network utilization. By increasing w_{post}, islanding becomes preferred over a wider uncertainty range as it provides the lowest dependency on σ. Again, this look-up table is specific to the assumed event center. The threshold uncertainty as well as the order of preventive actions may vary for other event centers.

IV. Conclusion

This article presented a risk assessment to weather-related power outages under spatial uncertainty and proposed a decision-making process that aids network operators on choosing among multiple options the best-performing preventive action to improve power grid resilience.

A novel uncertainty-driven quantification of performance loss was presented, assessing preventive actions based on two aspects: First, the preevent impact of preventive actions and any reductions in network utilization after applying the action. Second, the postevent reduction of the impact of individual or simultaneous line outages after applying a preventive action. Weighting factors were introduced to reflect the different influence of pre- and postevent impact on the decision-making, and tune the tradeoff between those.

The methodology was demonstrated using three different preventive actions, namely requiring the traditional *N*-1 criterion only for a single line (1–1 criterion), isolating a single area, and sectionalizing the entire network into multiple islands. These actions were compared to the traditional *N*-1 criterion. Simulation results obtained from the IEEE 30-bus test network and a model of the German transmission network showed that the decision-making methodology effectively ranks the available actions for every level of spatial uncertainty, considers pre- and postevent performance loss incurred by the actions as well as individual weighting factors, and provides insights into the generalized, underlying principles of how preventive actions improve resilience. The methodology could be split into three stages, allowing for the computationally expensive calculation of lost load for different event outcomes to be performed offline. The decision, which needs to consider quickly evolving and changing conditions, can be made online in real-time. Simple look-up tables, which propose a best-performing action, were presented, but it was discussed how the proposed performance loss may also be used to generate training data for more comprehensive machine learning algorithms, such as decision trees or support vector machines. Performance loss may also be used as an objective function in a formal optimization problem, which identifies the action that minimizes performance loss subject to uncertainty. While there would no longer be a need for look-up tables, solving the optimization problem still requires risk-based and uncertainty-dependent quantification of pre- and postevent performance loss as proposed by this methodology. The results therefore assist network operators in shifting from cost-intensive deterministic reliability criteria, e.g., the traditional *N*-1 criterion, toward a more optimal probabilistic approach, preventing cascading failures, and improving power grid resilience. Future work of the authors will look into evaluating the practicality and improving the effectiveness of the methodology using historical data.

References

[1] D. P. Nedic, I. Dobson, D. S. Kirschen, B. A. Carreras, and V. E. Lynch, "Criticality in a cascading failure blackout model," *Int. J. Elect. Power Energy Syst.*, vol. 28, no. 9, pp. 627–633, 2006.

[2] *Executive Office of the President*, "Economic benefits of increasing electric grid resilience to weather outages," The White House Office of Science and Technology, Aug. 2013.

[3] P. Hines, J. Apt, and S. Talukdar, "Trends in the history of large blackouts in the United States," in *Proc. IEEE Power Energy Soc. Gen. Meeting, Convers. Del. Elect. Energy 21st Century*, vol. 15213, 2008, pp. 1–8.

[4] M. Panteli and P. Mancarella, "The Grid: Stronger, bigger, smarter?: Presenting a conceptual framework of power system resilience," *IEEE Power Energy Mag.*, vol. 13, no. 3, pp. 58–66, May/Jun. 2015.

[5] E. Heylen, M. Ovaere, S. Proost, G. Deconinck, and D. Van Hertem, "A multi-dimensional analysis of reliability criteria: From deterministic N - 1 to a probabilistic approach," *Electric Power Syst. Res.*, vol. 167, pp. 290–300, 2019.

[6] Australian Energy Market Operator, "Black system, South Australia, 28 Sep. 2016," Melbourne, Australia, 2017.

[7] North American Electric Reliability Corporation, "Hurricane IRMA event analysis report," Atlanta, GA, USA, Aug. 2018.

[8] E. Ciapessoni, D. Cirio, G. Kjølle, S. Massucco, A. Pitto, and M. Sforna, "Probabilistic risk-based security assessment of power systems considering incumbent threats and uncertainties," *IEEE Trans. Smart Grid*, vol. 7, no. 6, pp. 2890–2903, Nov. 2016.

[9] L. Haarla, O. Mäkelä, G. Brønmo, K. Johansen, P.-F. Bach, and G. Kjølle, "Generally accepted reliability principle with uncertainty modelling and through probabilistic risk assessment: Current practices, drivers and barriers for new reliability standards," 2014, Accessed: May 15, 2019. [Online]. Available: https://www.sintef.no/globalassets/project/garpur/deliverables/garpur-d1.2-current-practices-drivers-and-barriers-for-new-reliability-standards.pdf

[10] R. Moreno, D. Pudjianto, and G. Strbac, "Integrated reliability and cost-benefit-based standards for transmission network operation," *Proc. Inst. Mech. Eng., Part O, J. Risk Rel.*, vol. 226, no. 1, pp. 75–87, 2012.

[11] R. Preece and J. V. Milanovic, "Assessing the applicability of uncertainty importance measures for power system studies," *IEEE Trans. Power Syst.*, vol. 31, no. 3, pp. 2076–2084, May 2016.

[12] M. Aien, A. Hajebrahimi, and M. Fotuhi-Firuzabad, "A comprehensive review on uncertainty modeling techniques in power system studies," *Renewable Sustain. Energy Rev.*, vol. 57, pp. 1077–1089, 2016.

[13] A. Soroudi and T. Amraee, "Decision making under uncertainty in energy systems: State of the art," *Renewable Sustain. Energy Rev.*, vol. 28, pp. 376–384, 2013.

[14] A. Gholami, F. Aminifar, and M. Shahidehpour, "Front lines against the darkness: Enhancing the resilience of the electricity grid through microgrid facilities," *IEEE Electrific. Mag.*, vol. 4, no. 1, pp. 18–24, Mar. 2016.

[15] B. Vatani, B. Chowdhury, S. Dehghan, and N. Amjady, "A critical review of robust self-scheduling for generation companies under electricity price uncertainty," *Int. J. Elect. Power Energy Syst.*, vol. 97, pp. 428–439, 2018.

[16] Y. Ren, P. N. Suganthan, and N. Srikanth, "Ensemble methods for wind and solar power forecasting–A state-of-the-art review," *Renewable Sustain. Energy Rev.*, vol. 50, pp. 82–91, 2015.

[17] M. de Jong, G. Papaefthymiou, and P. Palensky, "A framework for incorporation of infeed uncertainty in power system risk-based security assessment," *IEEE Trans. Power Syst.*, vol. 33, no. 1, pp. 613–621, Jan. 2018.

[18] Z. Bie, Y. Lin, G. Li, and F. Li, "Battling the extreme: A study on the power system resilience," *Proc. IEEE*, vol. 105, no. 7, pp. 1253–1266, Jul. 2017.

[19] M. Panteli, D. N. Trakas, P. Mancarella, and N. D. Hatziargyriou, "Boosting the power grid resilience to extreme weather events using defensive Islanding," *IEEE Trans. Smart Grid*, vol. 7, no. 6, pp. 2913–2922, Nov. 2016.

[20] M. Noebels and M. Panteli, "Assessing the effect of preventive Islanding on power grid resilience," in *Proc. IEEE Milan PowerTech*, 2019, pp. 1–6.

[21] C. Chen, J. Wang, F. Qiu, and D. Zhao, "Resilient distribution system by microgrids formation after natural disasters," *IEEE Trans. Smart Grid*, vol. 7, no. 2, pp. 958–966, Mar. 2016.

[22] Z. Li, M. Shahidehpour, F. Aminifar, A. Alabdulwahab, and Y. Al-Turki, "Networked microgrids for enhancing the power system resilience," *Proc. IEEE*, vol. 105, no. 7, pp. 1289–1310, Jul. 2017.

[23] M. Nazemi, M. Moeini-Aghtaie, M. Fotuhi-Firuzabad, and P. Dehghanian, "Energy storage planning for enhanced resilience of power distribution networks against earthquakes," *IEEE Trans. Sustain. Energy*, vol. 11, no. 2, pp. 795–806, Apr. 2020.

[24] J. Confrey, A. H. Etemadi, S. M. Stuban, and T. J. Eveleigh, "Energy storage systems architecture optimization for grid resilience with high penetration of distributed photovoltaic generation," *IEEE Syst. J.*, vol. 14, no. 1, pp. 1135–1146, Mar. 2020.

[25] T. Ding, Y. Lin, Z. Bie, and C. Chen, "A resilient microgrid formation strategy for load restoration considering master-slave distributed generators and topology reconfiguration," *Appl. Energy*, vol. 199, pp. 205–216, 2017.

[26] H. Khazraj *et al.*, "Optimal operational scheduling and reconfiguration coordination in smart grids for extreme weather condition," *IET Gener., Transmiss. Distrib.*, vol. 13, no. 15, pp. 3455–3463, 2019.
[27] P. Dehghanian, S. Aslan, and P. Dehghanian, "Maintaining electric system safety through an enhanced network resilience," *IEEE Trans. Ind. Appl.*, vol. 54, no. 5, pp. 4927–4937, Sep.-Oct. 2018.
[28] Y. P. Fang and G. Sansavini, "Optimum post-disruption restoration under uncertainty for enhancing critical infrastructure resilience," *Rel. Eng. Syst. Saf.*, vol. 185, pp. 1–11, 2019.
[29] N. Senroy, G. T. Heydt, and V. Vittal, "Decision tree assisted controlled Islanding," *IEEE Trans. Power Syst.*, vol. 21, no. 4, pp. 1790–1797, Nov. 2006.
[30] R. Eskandarpour and A. Khodaei, "Machine learning based power grid outage prediction in response to extreme events," *IEEE Trans. Power Syst.*, vol. 32, no. 4, pp. 3315–3316, Jul. 2017.
[31] M. A. Karim, J. Currie, and T. T. Lie, "Distributed machine learning on dynamic power system data features to improve resiliency for the purpose of self-healing," *Energies*, vol. 13, no. 13, 2020, Art. no. 3494.
[32] M. Panteli, P. Mancarella, D. N. Trakas, E. Kyriakides, and N. D. Hatziargyriou, "Metrics and quantification of operational and infrastructure resilience in power systems," *IEEE Trans. Power Syst.*, vol. 32, no. 6, pp. 4732–4742, Nov. 2017.
[33] S. Ma, B. Chen, and Z. Wang, "Resilience enhancement strategy for distribution systems under extreme weather events," *IEEE Trans. Smart Grid*, vol. 9, no. 2, pp. 1442–1451, Mar. 2016.
[34] B. Taheri, A. Safdarian, M. Moeini-Aghtaie, and M. Lehtonen, "Distribution systems resilience enhancement via pre- and post-event actions," *IET Smart Grid*, vol. 2, no. 4, pp. 549–556, 2019.
[35] J. Salomon, M. Broggi, S. Kruse, S. Weber, and M. Beer, "Resilience decision-making for complex systems," *ASCE-ASME J. Risk Uncertainty Eng. Syst., Part B, Mech. Eng.*, vol. 6, no. 2, pp. 1–11, 2020.
[36] M. Leutbecher and T. N. Palmer, "Ensemble forecasting," *J. Comput. Phys.*, vol. 227, no. 7, pp. 3515–3539, 2008.
[37] Met Office, "Beaufort wind force scale," Accessed: Oct. 19, 2020. [Online]. Available: https://www.metoffice.gov.uk/weather/guides/coast-and-sea/beaufort-scale
[38] M. R. Jamieson, G. Strbac, and K. R. Bell, "Quantification and visualisation of extreme wind effects on transmission network outage probability and wind generation output," *IET Smart Grid*, vol. 3, no. 2, pp. 112–122, 2020.
[39] L. Ding, F. M. Gonzalez-longatt, P. Wall, and V. Terzija, "Two-step spectral clustering controlled Islanding algorithm," *IEEE Trans. Power Syst.*, vol. 28, no. 1, pp. 75–84, Feb. 2013.
[40] R. J. Sánchez-García *et al.*, "Hierarchical spectral clustering of power grids," *IEEE Trans. Power Syst.*, vol. 29, no. 5, pp. 2229–2237, Sep. 2014.
[41] J. Quirós-Tortós, R. Sánchez-García, J. Brodzki, J. Bialek, and V. Terzija, "Constrained spectral clustering-based methodology for intentional controlled islanding of large-scale power systems," *IET Gener., Transmiss. Distrib.*, vol. 9, no. 1, pp. 31–42, 2015.
[42] H. Guo, C. Zheng, H. H. C. Iu, and T. Fernando, "A critical review of cascading failure analysis and modeling of power system," *Renewable Sustain. Energy Rev.*, vol. 80, pp. 9–22, 2017.
[43] W. Medjroubi, C. Matke, and D. Kleinhans, "SciGRID–an open source reference model for the European transmission network (v0.2)," 2015. Accessed: Oct. 31, 2021. [Online] Available: https://www.scigrid.de
[44] T. Brown, J. Hörsch, and D. Schlachtberger, "PyPSA: Python for power system analysis," *J. Open Res. Softw.*, vol. 6, no. 1, pp. 1–10, 2018.

Matthias Noebels (Student Member, IEEE) received the M.Sc. degree in physics from the University of Konstanz, Konstanz, Germany, in 2015. He is currently working toward the Ph.D. degree in electrical engineering with the Centre for Doctoral Training in Power Networks, The University of Manchester, Manchester, U.K.

His expertise lies in resilience analysis of power networks as well as developing strategies that can enhance resilience in case of natural hazards such as extreme weather.

Jairo Quiros-Tortos (Senior Member, IEEE) received the Ph.D. degree in electrical engineering from The University of Manchester, Manchester, U.K., in 2014.

He is currently a Professor in energy systems with the University of Costa Rica, San Pedro, Costa RIca. He has executed more than 15 industrial projects as consultant for multilateral development banks and international organizations. He has authored more than 80 journals and conferences in the field of energy systems and more than 30 technical reports. His research interests include building, modeling, and analyzing long-term decarbonization strategies to support climate change policy, primarily in the energy sector, as well as its link with other sectors.

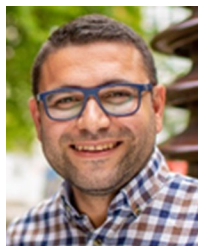

Mathaios Panteli (Senior Member, IEEE) received the M.Eng. degree in electrical and computer engineering from the Aristotle University of Thessaloniki, Thessaloniki, Greece, in 2009, and the Ph.D. degree in electrical power engineering from The University of Manchester, Manchester, U.K., in 2013.

He is currently an Assistant Professor with the Department of Electrical and Electronic Engineering, University of Cyprus. His main research interests include techno-economic reliability, resilience and flexibility assessment of future low-carbon energy systems, grid integration of renewable energy sources and integrated modelling and analysis of co-dependent critical infrastructures.

Dr. Panteli is an IET Chartered Engineer (CEng), the Chair of the CIGRE Working Group C4.47 "Power System Resilience" and an active member of multiple IEEE working groups. He is also the recipient of the prestigious 2018 Newton Prize.